

# Combined Laser Beam Braze-Welding Process for Fluxless Al-Cu Connections

T. Solchenbach, P. Plapper

Laser Technology Competence Centre, Research Unit in Engineering Science, University of Luxembourg

## Abstract

A combined laser beam welding and brazing process for Al-Cu connections in overlap configuration is investigated. Aluminium and copper for electric and electronic application is used for experiments without surface treatment or activation, e.g. by flux. Although Al and Cu have been considered as “not weldable”, the possibility of a thermal joining process, i.e., the weld-brazing, was proved. The inevitable formation of intermetallic compounds at the interfacial region was reduced to less than 4  $\mu\text{m}$ . Shear strength up to 51 MPa was achieved. A detailed fracture analysis has shown that the copper-rich intermetallic phase is the metallurgical weakest point due to the distinctive brittleness, even though the Al-rich  $\theta$ -phase is several times thicker.

## Keywords

Combined Laser Beam Brazing and Welding, Dissimilar Materials, Intermetallic Compounds

## 1 INTRODUCTION

In the field of electromobility the demand for higher power and energy density is growing, especially in the field of battery technology. To fulfil the stringent technical requirements, such as excellent mechanical, thermal, electric and corrosive characteristics, novel joining technologies for electric connections are needed.

A battery module assembly task is exemplary shown in figure 1 where the terminals of several pouch type Li-Ion cells have to be interconnected.

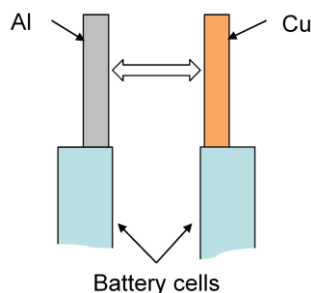


Figure 1 - Battery module assembly

However, aluminium and copper have to be considered as “not weldable” with conventional thermal joining methods due to the low solubility of both elements and the formation of several intermetallic compounds (IMC), see table 1, [1].

The distinctive brittleness of the IMCs drastically reduces the mechanical strength of such joints, whereas the hardness of the compounds increases with the amount of copper [2]. In addition, IMCs can significantly reduce the electrical conductivity of joints.

Different joining methods have been subject of research, i.e. electron beam welding, friction stir

welding, ultrasonic welding or roll cladding, e.g. [3], [4]. Beside very complex equipment (vacuum, handling devices, etc.) and beam deflections by magnetic fields, the work piece geometry is still restricted to thick and flat sheets.

Laser beam welding is another promising technology for joining dissimilar materials as reported in [5], [6] and [7]. As both metals are melted during the process, a high intermixture with large IMC seams distributed in the complete joint area was observed which has negative impact on the joint strength.

Temporal and spatial beam oscillation has been investigated in order to minimize the intermetallic seam width [8]. Furthermore the usage of additional materials as buffer layer, e.g. silver, in combination with modulated laser pulses was investigated [9].

As all mentioned approaches are based on deep penetration welding, the main disadvantage is the intermixture of both aluminium and copper and therewith the uncontrollable formation of intermetallic compounds to more than 10  $\mu\text{m}$ , [6].

## 2 COMBINED LASER WELDING AND BRAZING PROCESS

To overcome this issue, a braze-welding process for Al-Cu connections is introduced. As known from steel-aluminium, titanium-aluminium and other dissimilar combinations, the different melting temperatures of dissimilar materials can be used for melting of only one component, e.g. [10] or [11]. In the present case, only the Al layer ( $T_{Melt} = 660\text{ }^{\circ}\text{C}$ ) will be melted, copper ( $T_{Melt} = 1084\text{ }^{\circ}\text{C}$ ) stays in solid state. Thus, for aluminium it is a welding, for copper a brazing process. First feasibility tests have shown the general applicability of the process, [12].

Phase	Composition	Crystal structure	Atoms per unit cell	Hardness HV (10 g)
$\gamma_2$	$\text{Al}_4\text{Cu}_9$	body-centered cubic	36 Cu, 16 Al	770
$\zeta_2$	$\text{Al}_3\text{Cu}_4$	Monoclinic	12 Cu, 9 Al	930
$\eta_2$	AlCu	Body-centered orthorhombic	10 Cu, 10 Al	905
$\theta$	$\text{Al}_2\text{Cu}$	Body-centered tetragonal	4 Cu, 8 Al	630

**Table 1** - Important intermetallic compounds in the Al-Cu system

With a controlled heat input during the process it is demonstrated, that the seam width of intermetallic compounds can be reduced leading to a more homogenous interface with good mechanical, corrosive and electrical properties, whereas the mechanical characteristics are the main focus of this paper.

For a similar setup as described in [10] with indirect heating of the Al layer by heat conduction, the required laser power would be very high due to the high thermal conductivity of copper. Therefore, the laser beam is directly irradiated on the Al surface, see Figure 2. For intensity reasons, a laser beam source with excellent focusability is used.

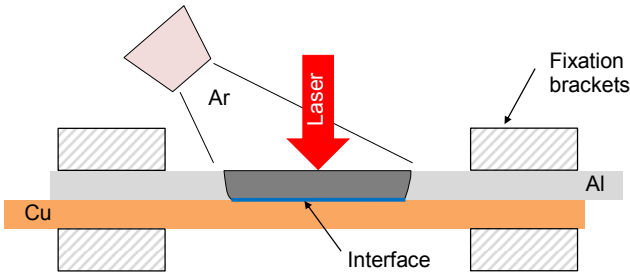


**Figure 2** - Combined laser welding and brazing process

To enlarge the joint area, a circular movement is superposed to the linear feed direction, see Figure 3.

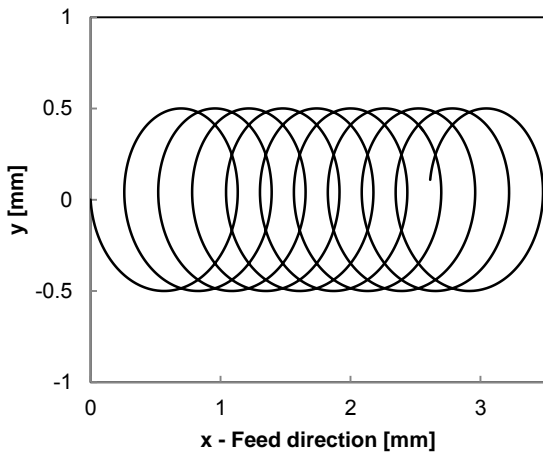


**Figure 3** - Superposed circular beam movement

The trajectory of the beam movement can be described according equation (1):

$$\begin{pmatrix} x(t) \\ y(t) \end{pmatrix} = \begin{pmatrix} -a \cdot \cos(2\pi ft) + vt + a_0 \\ -a \cdot \sin(2\pi ft) \end{pmatrix} \quad (1)$$

with

$a$  amplitude of circular movement [mm]

$a_0$  starting position at  $t = 0$  [mm]

$f$  repetition frequency [ $\text{s}^{-1}$ ]

$v$  feed rate in  $x$  [ $\text{mm s}^{-1}$ ]

From [13] and [14] it is known that oscillation frequencies up to 2 kHz at amplitudes up to 2 mm can influence the melt pool shape. For welding experiments with Al, resonance phenomena are reported for frequencies between 500 and 700 Hz, [14]. Thus, an amplitude of 0.5 mm at a frequency of 100 Hz is chosen for the present experiments, which represents the lower end of the frequency range. In the following, the overlap  $n$  is the main parameter of investigations.

From Figure 3 it can be seen that the overlap  $n$  in  $x$ -direction for  $y = 0$  between two cycles can be defined to:

$$n = \frac{x\left(\frac{T}{2}\right) - x(2T)}{x\left(\frac{T}{2}\right) - x(T)} \quad (2)$$

with  $T$  representing the periodic time:

$$T = \frac{1}{f} \quad (3)$$

Using equation (1), equation (2) can be written as:

$$n = \frac{4a - 3vT}{4a - vT} = \frac{4a - 3\frac{v}{f}}{4a - \frac{v}{f}} \quad (4)$$

In analogy to pulsed laser beam welding, the overlap between two circular movements is expected to be between 0.7 and 0.95 [15]. Thus, feed rates between 4 and 26  $\text{mm s}^{-1}$  can be accomplished.

### 3 EXPERIMENTAL SETUP

A single mode Trumpf TruFiber fibre laser at a wavelength of  $\lambda = 1070 \text{ nm}$  with beam quality of  $M^2 = 1.03$  with a continuous power of 400 W is used in combination with a Scanlab HS20 2D scanner head with an optical magnification of 2.8x. Thus, a spot diameter of 30  $\mu\text{m}$  can be obtained with the focus on the Al surface.

For the experiments SF-Cu (C10100) and Al 99.5 (EN AW1050A), both in half-hard state with a thickness of each 500  $\mu\text{m}$  are used. The samples are mounted in overlap configuration between Al fixation brackets. This set up provides a thermal conductive fixation for high temperature gradients during the joining process.

The samples are cleaned with an acetone solution. To avoid any pre-process work, surface treatment or activation, e.g. by flux, are not utilized.

According to Figure 2, Argon shielding gas of quality 4.6 is applied by a four tube nozzle perpendicular to the feed direction at a flow of 12 l/min.

After the joining process, the samples were analysed with optical and electron microscopes and tested for mechanical strength per AWS C3.2:2008 [16]. Therefore, the specimens are machined to a test length of 16 mm (seam length 35 mm) in order to avoid a possible influence of the run-in and run-out areas of the laser process.

A scope of 10 samples per parameter set is chosen.

### 4 RESULTS AND DISCUSSION

#### 4.1 Microscopic analysis

Basically three different seam structures have been observed, see Figure 4.

For optimal process parameters a homogenous interface between Al and Cu must be formed (b). If the power and overlap are reduced, the interface is not fully developed and voids appear (a). If the power and overlap are increased the laser beam penetrates into the copper layer and melts it (c). The experimental results represent a process window, see Figure 5.

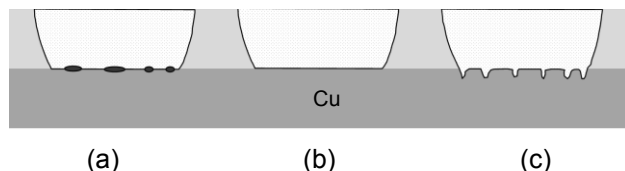


Figure 4 - Possible seam structures

As no surface treatment or activation is used for these experiments, the aluminium-oxide layer at the Al-Cu interface has to be melted during the process. As Al-oxide has a higher melting temperature (2050 °C) compared to pure aluminium, the transition from (b) to (a) or (c) proceeds in a very narrow band of overlap  $n$  and laser power  $P$ .

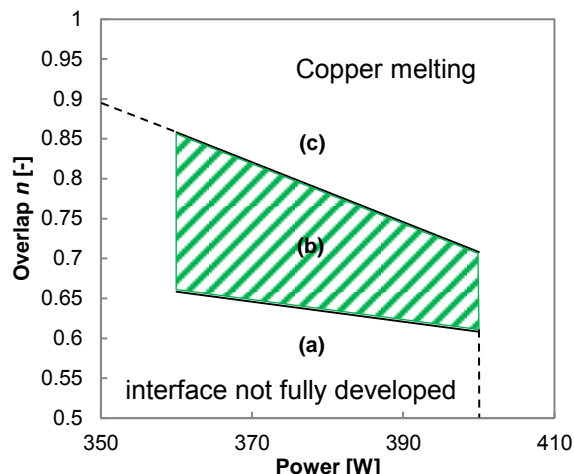


Figure 5 - Process window for homogenous interface

Thus, even for case (b), the interface is formed in a wavy manner which can be explained by an inhomogeneous energy deposition, see longitudinal section in Figure 6.

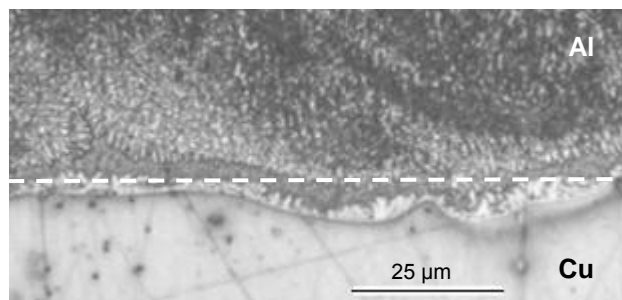


Figure 6 - Wavy interface in longitudinal section

For case (b), the joint between Al and Cu is based on pure diffusion bonding with only very small effect of mechanical interlocking.

The fusion zone can be divided into four different areas. In the intermetallic  $\text{Al}_x\text{Cu}_y$  phase hem, two different types of compounds can be assessed, see Figure 7.

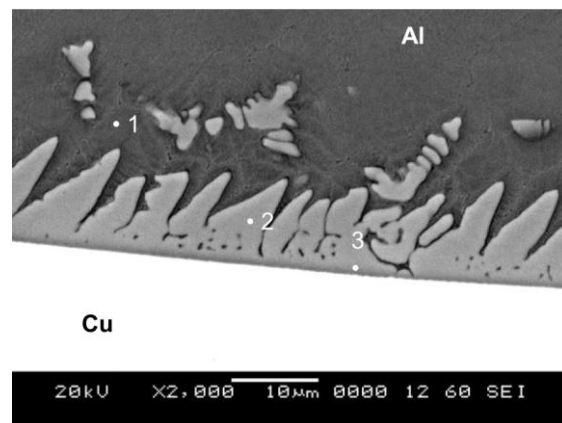


Figure 7 - SEM image of the interface

The Al-rich phase with its typical dendritic growth structure appears in light grey, the dark-grey Cu-rich phase, however, is several times thinner (up to 500 nm) than the Al-rich phase. This can be explained by different diffusion rates [17].

The chemical composition of the interface was analysed by means of SEM/EDX methods, see Table 2. In the interfacial region, the Al base material is doped with intermetallic compounds, see marker "1" in Figure 8. With 60.89 weight-% Al the left eutectic compound was detected, as compared to Figure 1.

	wt.-% Al	wt.-% Cu	
1	60.89	39.11	
2	44.63	55.37	Al <sub>2</sub> Cu (θ)

Table 2 - SEM/EDX analysis

With 44.63 wt.-% Al, the Al-rich intermetallic compound is the Al<sub>2</sub>Cu (θ) phase, see marker "2". However, the composition of the Cu-rich intermetallic phase "3" has not been investigated yet.

The average size of the IMC seam width was observed by microscopic measurements, see Figure 8. A seam width of 0 correlates to a not fully developed interface, see Figure 5 (a). For case (b) and (c) each the maximum seam width is represented. For increasing power  $P$  and overlap  $n$ , thus with higher energy input, the intermetallic seam grows exponentially. However, the seam width has been reduced to less than 4 μm for most parameters which is, compared to literature, a reduction of more than factor 2.

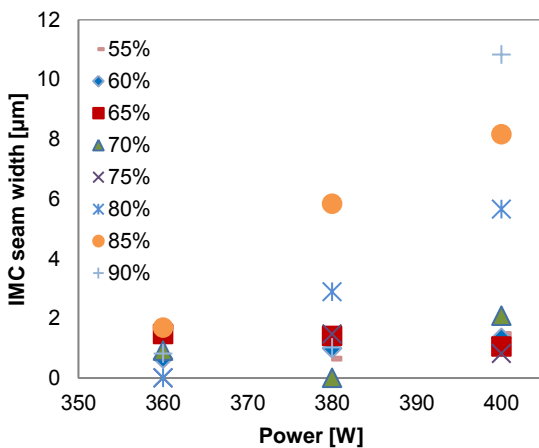


Figure 8 - Average IMC seam width over power; a seam width of 0 correlates to a not fully developed interface

#### 4.2 Seam irregularities

For all parameter sets hot cracks were detected, see Figure 9, arrow markers. The position of the cracks and the growth direction indicate a distinctive

brittleness and the influence of different thermal expansion coefficients of Al and Cu which leads to stress in the weld bead.

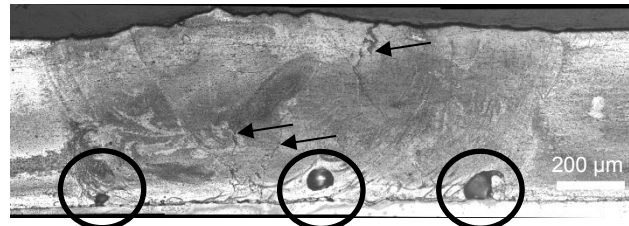


Figure 9 - Hot crack and pore formation ( $P = 400 \text{ W}$ ,  $n = 0.65$ )

Furthermore, in the interfacial region, pores were assessed which can be explained by the turbulent melt flow during the process, see Figure 9, circle markers.

The keyhole in the aluminium layer can collapse due to the pores which then leads to reduced bonding quality between 60 and 80 % (ratio between bonded and expected area).

#### 4.3 Mechanical characteristics

The mechanical characteristics are the main subject of the present investigations.

For shear tests basically two different failure modes can occur:

- The specimen fails in the heat affected Al base material,
- The specimen fails at the Al-Cu interface.

As most of the specimens are broken in the interface, it is possible to characterize the interface strength.

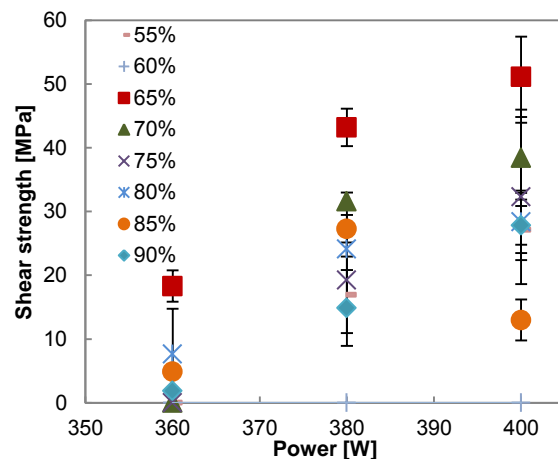


Figure 10 - Results of shear tests

Figure 10 illustrates the results of shear tests. A maximum shear strength of 51 MPa was observed for 400 W and 65 % overlap. Compared to Figure 5, these parameters describe the lower limit at the changeover from (b) to (a). For reduced power  $P$  or the overlap  $n$ , voids appear at the interface and the strength is reduced. With increasing  $P$  or  $n$ , the size



of the intermetallic phase increases which then also reduces the joint strength.

Due to high deviations in the strength values, caused by the instable bonding quality, a clear relation between intermetallic seam width and shear strength cannot be drawn, see figure 11. But, for decreasing seam width, a clear tendency towards higher strength can be seen. However, also here the very narrow changeover from case (b) to (a) is obvious.

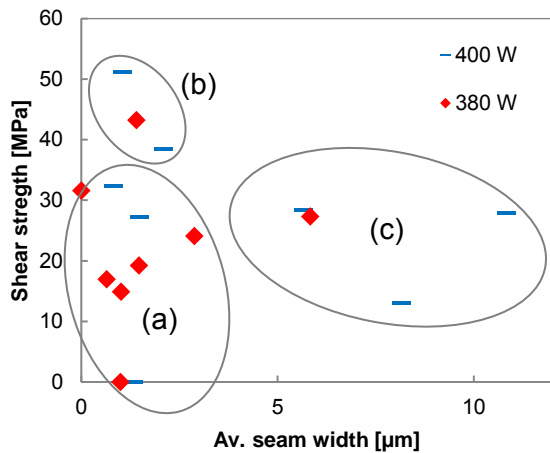


Figure 11 - Shear strength over ICM seam width

Based on the shear tests, the fracture of the specimen is highly brittle with little ductile strain, see Figure 12.

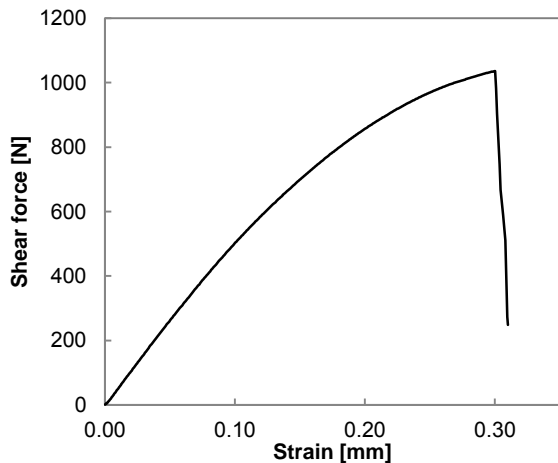


Figure 12 - Brittle fracture in the interface ( $P = 400 \text{ W}$ ,  $n = 0.65$ )

A detailed fracture analysis of the broken samples confirms this result. On the micrograph in Figure 13 the wavy interface structure can be identified, as compared to Figure 6. In area A the formation of dimples and distinctive slip lines indicate a more ductile fracture, see Figure 14.

For cross section B-B, a brittle trans-crystalline fracture on the copper side can be clearly detected. Even though the width of the Cu-rich phase is much

smaller than the  $\theta$ -phase, the fracture of the specimen took place on the copper side. Thus, the Cu-near IMC is the metallurgical weakest area of the interface.

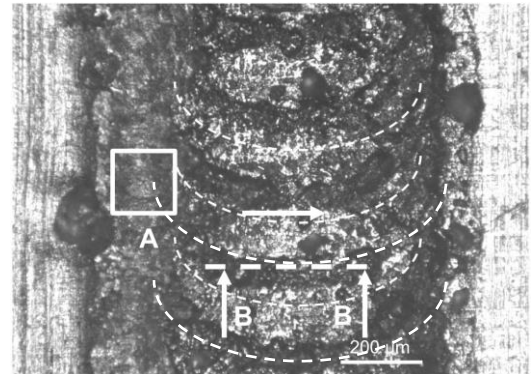
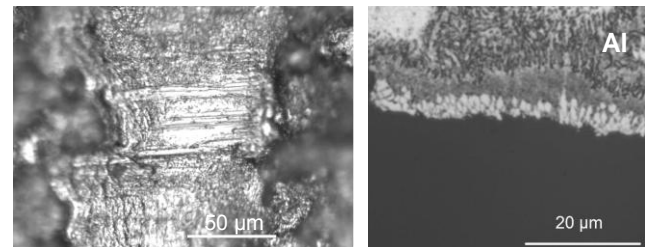


Figure 13 - Micrograph of a broken Al-Cu sample (Al side,  $P = 400 \text{ W}$ ,  $n = 0.65$ )



A: Ductile fracture with slip lines      B-B: brittle fracture at the Cu-near IMC

Figure 14 - Different types of fracture

## 5 CONCLUSIONS

A combined laser beam braze-welding process for fluxless Al-Cu connections has been investigated. A fibre laser in combination with a 2D scanner optic was used to enable superposed circular beam movements.

By controlling the laser power and the geometrical overlap of a superposed circular beam movement, the optimal process parameters have been found experimentally.

It was proved that the formation of intermetallic compounds can be strongly reduced which leads to high shear strength up to 51 MPa at the interface. The upper limit for intermetallic compounds at Al-Cu connections is measured to 4  $\mu\text{m}$  which exceeds literature values of 10  $\mu\text{m}$ .

Although the Cu-rich intermetallic compound is several times thinner than the Al-rich  $\theta$ -phase, the fracture of the specimen takes place at the Cu side.

Furthermore, hot cracks and pores have been detected which can be explained by irregular gas shielding and the turbulent melt flow of the fluid aluminium.

For the future, experiments with temporal power modulation are envisioned in order to combine a high intense laser beam with a low overall heat input. Also the superposed beam movement will be assessed in detail. With these improvements a further reduction of the IMC seam width and a more homogenous and adapted energy deposition is expected. Furthermore, the fatigue as well as the electric properties of the joints have to be proved.

## 6 ACKNOWLEDGEMENTS

The authors would like to thank the Luxembourgish Ministère de l'Economie et du Commerce extérieur, the Fonds national de la recherche FNR Luxembourg and the CRP Henri Tudor AMS.

## 7 REFERENCES

- [1] Pohle, C., 1999, Schweißen von Werkstoffkombinationen, DVS Verlag
- [2] Westbrook, J.H., Fleischer, R.L. 2000, Structural Applications of Intermetallic Compounds, John Wiley & Sons
- [3] Sun, Z., Karppi, R., 1996, The application of electron beam welding for the joining of dissimilar metals: an overview, Journal of Materials Processing Technology, 59, 257-267
- [4] Lee, D, Kannatey-Asibu, Jr., E., and Cai, W., "Ultrasonic Welding Simulations for Multiple, Thin and Dissimilar Metals, Proceedings of ASME International Symposium on Flexible Automation, St. Louis, June 18-20, 2012.
- [5] Klages, K., 2006, Laserstrahl-Mikroschweißen ungleicher Metalle durch Nahtschweißen mit gepulsten Nd:YAG-Lasern, Shaker Verlag
- [6] Theron, M., Van Rooyen, C., Ivanchev, L. H., 2007, CW ND:YAG laser welding of dissimilar sheet metals, ICALEO congress proceedings
- [7] Mai, T.A., Spowage, A.C., 2004, Characterization of dissimilar joints in laser welding of steel–kovar, copper–steel and copper–aluminium, Materials Science and Engineering A, 374, 224-233
- [8] Kraetzsch, M., Standfuss, J., Klotzbach, A., Kaspar, J., Brenner, B., Beyer, E., 2011, Laser beam welding with high-frequency beam oscillation: welding of dissimilar materials with brilliant fiber lasers, Physics Procedia 12, 142-149
- [9] Weigl, M., Albert, F., Schmidt, M., 2011, Enhancing the ductility of laser-welded copper-aluminium connections by using adapted filler materials, Physics Procedia 12, 335-341
- [10] Radscheit, C. R., 1997, Laserstrahlfügen von Aluminium mit Stahl, BIAS Verlag
- [11] Wagner, F., Zerner, I., Kreimeyer, M., Sepold, G., 2001, Phasenbildung beim Laserstrahlfügen von Fe/Al-Verbindung, DVS-Berichte, 212, 03-98
- [12] T. Solchenbach, P. Plapper, 2012, Laser Diffusion Welding of Al-Cu Connections", EALA 2012 conference, Bad Nauheim, Germany
- [13] Gedicke, J., Olowinsky, A., Artal, J., Gillner, A., 2007, Influence of temporal and spatial laser power modulation on melt pool dynamics, ICALEO congress proceedings
- [14] R. Poprawe, 2004, Hochfrequentes Strahlpendeln zur Erhöhung der Prozessstabilität beim Laserstrahlschweißen mit hoher Schmelzbaddynamik, Intermediate report from AiF 13.600N project
- [15] Ready, J. F., Farson, D. F., 2001, LIA Handbook of laser materials processing, Magnolia Publishing
- [16] American Welding Society, 2008, Standard method for evaluating the strength of brazed joints, AWS standard
- [17] Funamizu, Y., Watanabe, K., 1971, Interdiffusion in the Al-Cu system, Trans. J I M, 12, 147-152

## 8 BIOGRAPHY



Tobias Solchenbach holds a M. Eng. degree in Automotive Engineering from the University of Applied Sciences Trier. He is currently PhD student at the University of Luxembourg. His main area of research interest is laser beam joining of dissimilar materials.



Peter Plapper obtained his PhD degree in Machine tools and Production Engineering (WZL) from the Technical University of Aachen (RWTH). Since 2010 he is Professor for Tool Machines and Production Technology at the University of Luxembourg